Linkage and Redox Isomerism in Ruthenium Complexes of Catecholate, Semiquinone, and *o*-Acylphenolate Ligands Derived from 1,2-Dihydroxy-9,10-anthracenedione (Alizarin) and Related Species: Syntheses, Characterizations, and Photophysics

Melvyn Rowen Churchill,* Kim M. Keil, Frank V. Bright,* Siddharth Pandey, Gary A. Baker, and Jerome B. Keister*

Department of Chemistry, University at Buffalo, the State University of New York, Buffalo, New York 14260-3000

Received May 19, 2000

The complexes $Ru(CO)_2L_2$(AL-2H) (AL = alizarin; L = PPh_3, $PCyc_3$, PBu_3, P(*m*-$NaSO_3C_6H_4)_3$), Ru(CO)(dppe)-(PBu_3)(AL-2H), and $RuH(CO)L_2$(AL-H) (L = PPh_3, $PCyc_3$), and $Ru(CO)_2L_2$(AR-2H) (AR = anthrarobin; L = PBu_3) were prepared by reactions of $Ru_3(CO)_{12}$, L, and AL, and the complexes $RuH(CO)(PPh_3)_2$(AL-H), RuH-$(CO)(PPh_3)_2$(QN-H) (QN = quinizarin), and $RuH(CO)(PPh_3)_2$(LQN-H) (LQN = leucoquinizarin) are prepared by reactions of $RuH_2(CO)(PPh_3)_3$ with AL or QN. The AL-2H and AR-2H ligands act as 1,2-catecholates, whereas the AL-H, QN-H, LQN-H ligands are 1,9-*o*-acylphenolate ligands. $RuH(CO)(PPh_3)_2$(AL-H) is characterized by X-ray crystallography. The electrochemistry of these complexes is examined, and the semiquinone complexes $[Ru(CO)_2L_2(AL\text{-}2H)]^+$ (L = PPh_3, $PCyc_3$, PBu_3) and $[Ru(CO)(dppe)(PBu_3)(AL\text{-}2H)]^+$ are generated by chemical oxidation and were characterized by EPR and IR spectroscopy. The photophysical properties are also reported.

Introduction

Metal complexes of alizarin[1] have been used as dyes for centuries. Ancient Egyptians extracted the compound from the root of the madder plant, and the discovery of a synthetic route in 1869 was a significant factor in the development of the German chemical industry.[2] Although the coordination chemistry of alizarin has received some attention, very few organometallic complexes have been reported. As ligands, alizarin and its substituted derivatives offer three features of interest to organometallic chemistry: (1) Alizarin can exhibit linkage isomerism, acting as a chelate via the 1,2- or the 1,9-oxygen atoms. (2) As a 1,2-chelate, it displays ligand-based redox chemistry. (3) The complexes are deeply (and beautifully) colored, allowing for applications of these compounds as optical sensor components or as molecular recognition elements. In this paper, we present the syntheses and characterizations of ruthenium complexes of the alizarinate ligand, demonstrating the ability of this ligand to act as a 1,2-catecholate, a 1,2-semiquinone, and an *o*-acylphenolate ligand. In a subsequent paper, we will describe analogous organometallic complexes of tri- and tetrahydroxy-9,10-anthracenediones.

Experimental Section

Starting Materials. Dichloromethane was distilled under nitrogen from calcium hydride before use. Alizarin (AL; 97%), quinizarin (QN), anthrarobin (AR technical grade, 85% purity), and tributylphosphine were purchased from Aldrich, and $Ru_3(CO)_{12}$ and 1,2-bis(diphenylphosphino)ethane (dppe) were obtained from Strem Chemical Co. Sodium tris(*m*-sulfonatophenyl)phosphine (TPPTS) was provided by Dr. Laura Francisco and Professor Jim Atwood. Other chemicals were of reagent grade purity and were used as received.

Physical Methods of Characterizations. Infrared spectra were recorded on a Nicolet Magna 550 spectrophotometer. ^{1}H NMR spectra were obtained on a Varian Associates Gemini 300 or VXR-400S instruments. ^{13}C NMR spectra were recorded either on the Gemini 300 or the VXR-400S instrument in deuteriochloroform and referenced to TMS. ^{31}P NMR spectra were recorded on the VXR-400S instrument in deuteriochloroform, and chemical shifts are reported relative to orthophosphoric acid. UV/visible spectra were acquired by using a Hewlett-Packard 8452A diode array spectrophotometer. EPR spectra were recorded on an IBM/Bruker ESP 300 X-band ESR spectrometer in dichloromethane solution; *g* values and hyperfine coupling constants were determined by spectral simulations using Bruker WINEPR SimFonia Version 1.25 software.

Electrochemistry. Cyclic voltammetric experiments were performed with Bioanalytical Systems (West Lafayette, IN) BAS-100W electrochemical analyzer. Measurements were made in accordance with standard techniques which included purging of solutions with nitrogen to exclude oxygen. Dichloromethane was freshly distilled from calcium hydride and stored under nitrogen. The supporting electrolyte was 0.1 M tetrabutylammonium tetrafluoroborate, TBATFB (Kodak; also prepared by ion exchange of tetrabutylammonium bromide with sodium tetrafluoroborate), which had been recrystallized three times from ethanol/water and vacuum-dried. The working electrode for experiments at relatively low scan rates was a platinum disk electrode (diameter 3 mm). For work at higher scan rates, and for some of the steady-state investigations, smaller platinum disks (BAS; diameters 100 and 10 μm) were employed. A platinum wire served as the auxiliary (counter) electrode. The concentrations of the analyte were 10^{-3} M unless stated otherwise. The reference electrode used was a Ag wire, and potentials were referenced to ferrocene or decamethylferrocene, added to the solutions. Compensation for resistive losses (*iR* drop) was employed for all measurements. All potentials are reported relative to the ferrocene/ferrocenium couple as 0 V.

Photophysical Measurements. (a) Materials. $Ru(bpy)_3^{2+}$ and rhodamine 6G were obtained from GFS Chemicals and Acros Organics,

(1) Throughout this paper the following abbreviations are used: alizarin (1,2-dihydroxy-9,10-anthracenedione), AL; anthrarobin (9,9-dihydro-1,2-dihydroxy-10-anthracenone), AR; quinizarin (1,4-dihydroxy-9,-10-anthracenedione), QN; leucoquinizarin (2,3-dihydro-9,10-dihydroxy-1,4-anthracenedione), LQN. The removal of one hydroxyl proton is indicated by "-H" and that of two hydroxyl protons as "-2H".

(2) Fieser, L. F. *J. Chem. Educ.* **1930**, *7*, 2609.

10.1021/ic000529x CCC: $19.00
Published on Web 11/17/2000

respectively. The solvents used were as follows: dichloromethane (Fisher Scientific; 99.9%), toluene (Aldrich; 99.8%, anhydrous), acetonitrile (Sigma-Aldrich; 99.9%, HPLC grade), chloroform (Fisher Scientific; 99.9%), cyclohexane (Acros Organics; 99+%, spectrophotometric grade), ethanol (Pharmco, dehydrated), dimethyl sulfoxide (Fisher Scientific; 99.9%), and doubly distilled deionized water (Millipore).

(b) Methods. All samples were subjected to multiple freeze−pump−thaw cycles to remove dissolved oxygen prior to data acquisition. Absorbance measurements were carried out on a Spectronic 1201 spectrophotometer (Spectronic Instruments, Rochester, NY) with a spectral band-pass of ±0.5 nm. The scan rate was typically 200 nm/min, and all spectra were blank-corrected.

Steady-state and time-resolved fluorescence experiments were performed with an SLM-AMINCO model 48000 MHF phase-modulation spectrofluorometer (Spectronic Instruments). The instrument and its capabilities have been described in detail elsewhere.[3]

Fluorescence quantum yields (Φ) were determined relative to an optically dilute reference fluorophore solution that exhibits a well-known fluorescence quantum yield (Φ_r).[4,5] The quantum yield standard used in this study was a degassed aqueous $Ru(bpy)_3^{2+}$ solution ($\Phi = 0.042 \pm 0.002$ at 25 °C).[6] Because there are characteristic MLCT absorbance bands that overlap the fluorescence, we corrected all emission profiles for secondary inner-filter effects.[7,8]

Magic angle polarization conditions were used for all excited-state intensity decay kinetic experiments to eliminate bias stemming from fluorophore rotational reorientation. Rhodamine 6G dissolved in water was used as the reference lifetime standard; its lifetime was assigned a value of 3.85 ns.[9] The excited-state fluorescence lifetime, τ, was recovered from the phase-modulation data by using a nonlinear least-squares software package purchased from Globals Unlimited (Urbana, IL). In all data analyses, we used the true uncertainty in each datum as the frequency weighting factor. Further details on phase-modulation fluorescence can be found elsewhere.[10]

For all results reported here, the excited-state fluorescence lifetimes were rigorously single exponential.

For any fluorophore, the radiative (k_r) and nonradiative ($\sum k_{nr}$) decay rates describe the deactivation kinetics following electronic excitation.[11] These decay rates are related to the fluorescence quantum yield, Φ, and the excited-state fluorescence lifetime, τ, by

$$k_r = \phi/\tau \quad (1)$$

$$\sum k_{nr} = (1 - \phi)/\tau \quad (2)$$

Syntheses. (a) $Ru(CO)_2(PBu_3)_2$(AL-2H) and $Ru(CO)_2(PBu_3)_2$(AR-2H). A solution of $Ru_3(CO)_{12}$ (54.6 mg, 85 μmol), PBu_3 (120 μL,481 μmol), and alizarin (62.8 mg, 262 μmol) in toluene (20 mL) was heated at reflux under an argon atmosphere for 10 h. The resulting purple solution was evaporated to dryness and the residue was applied as a dichloromethane solution to a silica gel preparative TLC plate. Elution with first dichloromethane and then 8% acetone in dichloromethane gave a beet-colored leading band, closely followed by an orange band. A second TLC separation with 8% acetone in dichloromethane yielded pure compounds, which were extracted with acetone/dichloromethane: Band 1, $Ru(CO)_2(PBu_3)_2$(AL-2H), 77.3 mg, 97 μmol, 40%; band 2, $Ru(CO)_2(PBu_3)_2$(AR-2H), 58.0 mg, 74 μmol, 31%.

$Ru(CO)_2(PBu_3)_2$(AL-2H): IR (hexanes) 2029.5 s, 1965.5 s cm^{-1}. ^1H NMR ($CDCl_3$) 8.22 (m, $J = 6.6$ Hz, 2 H), 7.60 (m, $J = 7.5$ Hz, 3 H), 6.58 (d, $J = 8.4$ Hz, 1 H), 1.71 (m, 12 H), 1.49 (br d, $J = 12$ Hz), 1.35 (pent, $J = 7$ Hz, 12 H), 0.87 (t, $J = 7.0$ Hz, 18 H) ppm; $^{13}C\{^1H\}$ NMR ($CDCl_3$) 198.3 (1 C), 198.0 (1 C), 182.8 (1 C), 182.6 (1 C), 173.1 (1 C), 167.3 (1 C), 137.1 (1 C), 135.3 (1 C), 132.8 (1 C), 132.2 (1 C), 127.0 (1 C), 126.7 (1 C), 123.5 (1 C), 121.6 (1 C), 120.4 (1 C), 117.3 (1 C), 25.9 (6 C), 25.1 (6 C), 23.7 (6 C), 14.2 (6 C) ppm; $^{31}P\{^1H\}$ NMR ($CDCl_3$) 20.0 (s) ppm. Anal. Calcd for $C_{40}H_{60}O_6P_2Ru$: C, 60.06; H, 7.56. Found: C, 59.90; H, 7.69.

$Ru(CO)_2(PBu_3)_2$(AR-2H): IR (hexanes) 2025.3 s, 1959.7 s cm^{-1}; ^1H NMR ($CDCl_3$) 8.32 (d, $J = 8.0$ Hz, 1 H), 7.58 (d, $J = 8.0$ Hz, 1 H), 7.41 (m, 3 H), 6.59 (d, $J = 8.4$ Hz, 1 H), 4.06 (s, 2 H), 1.68 (br, 12 H), 1.48 (br, 12 H), 1.34 (m, 12 H), 0.89 (t, $J = 7$ Hz, 18 H) ppm; $^{13}C\{^1H\}$ NMR ($CDCl_3$) 198.8 (1 C), 198.4 (1 C), 184.2 (1 C), 167.2 (1 C), 157.2 (1 C), 142.0 (1 C), 134.2 (1 C), 131.6 (1 C), 129.1 (1 C), 127.9 (1 C), 127.3 (1 C), 126.7 (1 C), 122.1 (1 C), 118.5 (1 C), 115.9 (1 C), 28.5 (1 C), 26.1 (6 C), 25.2 (6 C), 23.6 (6 C), 14.4 (6 C) ppm; $^{31}P\{^1H\}$ NMR ($CDCl_3$) 19.4 (s) ppm. Anal. Calcd for $C_{40}H_{62}O_5P_2Ru$: C, 61.13; H, 7.95. Found: C, 61.31; H, 7.96.

(b) $Ru(CO)_2(PPh_3)_2$(AL-2H) and $RuH(CO)(PPh_3)_2$(AL-H). A solution of $Ru_3(CO)_{12}$ (110.0 mg, 173 μmol), PPh_3 (296 mg, 1130 μmol), and alizarin (128 mg, 533 μmol) in toluene (30 mL) was heated at reflux under an argon atmosphere for 9 h. The resulting solution was evaporated to dryness, and the residue was applied as a dichloromethane solution to silica gel preparative TLC plates. Elution with dichloromethane gave a yellow leading band, followed by one green, one brown, and two purple bands. Extraction of the green band with ethyl acetate gave 77.8 mg, 16.9%, of $RuH(CO)(PPh_3)_2$(AL-H). Extraction of the purple bottom purple band gave 197.3 mg, 41.5%, of $Ru(CO)_2(PPh_3)_2$(AL-2H).

$RuH(CO)(PPh_3)_2$(AL-H): IR (CH_2Cl_2) 1920.7 vs cm^{-1}; ^1H NMR ($CDCl_3$) 8.12 (dd, $J = 2$, 7 Hz, 1 H), 8.02 (dd, $J = \sim 2$, 7 Hz, 1 H), 7.6 (m, H), 7.2 (m, 19 H), 6.99 (s, 1 H), 6.49 (d, $J = 8$ Hz, 1 H), −13.99 (t, $J = 19$ Hz, 1 H) ppm, minor isomer hydride at −14.13 (t, $J = 19$ Hz) ppm, major/minor ~12; $^{31}P\{^1H\}$ NMR ($CDCl_3$) 45.0 (s) ppm. Anal. Calcd for $C_{51}H_{38}O_5P_2Ru$: C, 68.53; H, 4.28. Found: C, 68.21; H, 4.20.

$Ru(CO)_2(PPh_3)_2$(AL-2H): IR (CH_2Cl_2) 2043.6 s, 1981.5 s cm^{-1}; ^1H NMR ($CDCl_3$) 8.34 (d, $J = 7.6$ Hz, 1 H), 8.14 (d, $J = 6.8$ Hz, 1 H), 7.66 (t, $J = 7.6$ Hz, 1 H), 7.58 (t, $J = 8.4$ Hz), 7.54 (m, 12 H), 7.28 (m, 18 H), 6.97 (d, $J = 8.4$ Hz, 1 H), 5.83 (d, $J = 8.0$ Hz, 1 H) ppm; $^{31}P\{^1H\}$ NMR ($CDCl_3$) 21.0 (s) ppm. Anal. Calcd for $C_{52}H_{36}O_6P_2Ru$: C, 67.90; H, 3.94. Found: C, 67.68; H, 3.82.

(c) $Ru(CO)_2(PCyc_3)_2$(AL-2H) and $RuH(CO)(PCyc_3)_2$(AL-H). A solution of $Ru_3(CO)_{12}$ (110 mg, 172 μmol), $PCyc_3$ (303 mg, 1018 μmol), and alizarin (131 mg, 546 μmol) in toluene (30 mL) was heated at reflux under an argon atmosphere for 12 h. The resulting solution was evaporated to dryness, and the residue was applied as a dichloromethane solution to silica gel preparative TLC plates. Elution with dichloromethane gave two major bands. Extraction of the red-brown top band with ethyl acetate gave 152 mg, 32%, of $RuH(CO)(PCyc_3)_2$(AL-H). Extraction of the blue-purple bottom band gave 135 mg, 27%, of $Ru(CO)_2(PCyc_3)_2$(AL-2H).

$RuH(CO)(PCyc_3)_2$(AL-H): IR (CH_2Cl_2) 1897.2 cm^{-1}; ^1H NMR ($CDCl_3$) 8.23 (m, 1 H), 8.16 (m, 1 H), 7.68 (m, 2 H), 7.66 (s, 1 H), 7.48 (d, $J = 7.6$ Hz, 1 H), 6.90 (d, $J = 7.6$ Hz, 1 H), 2.1−0.8 (66 H), −15.15 (t, $J = 19.6$ Hz, 1 H) ppm; $^{31}P\{^1H\}$ NMR ($CDCl_3$) 43.5 (s) ppm. Anal. Calcd for $C_{51}H_{74}O_5P_2Ru$: C, 65.86; H, 8.02. Found: C, 65.86; H, 8.25.

$Ru(CO)_2(PCyc_3)_2$(AL-2H): IR (CH_2Cl_2) 2028.6 s, 1962.1 s cm^{-1}; ^1H NMR ($CDCl_3$) 8.23 (t, $J = 7$ Hz, 1 H), 8.22 (t, $J = 7$ Hz, 1 H), 7.62 (d, $J = 8$ Hz, 1 H), 7.58 (m, 2 H), 6.52 (d, $J = 8$ Hz, 1 H), 2.2−1.0 (m, 66 H) ppm; $^{31}P\{^1H\}$ NMR ($CDCl_3$) 37.2 (s) ppm. Anal. Calcd for $C_{52}H_{72}O_6P_2Ru$: C, 65.32; H, 7.59. Found: C, 65.05; H, 7.88.

(d) $Ru(CO)_2(P(O\text{-}i\text{-}Pr)_3)_2$(AL-2H): A solution of $Ru_3(CO)_{12}$ (100 mg, 156 μmol) and alizarin (115 mg, 479 μmol) in toluene (25 mL) was heated at reflux under an argon atmosphere for 4.5 h. Then $P(O\text{-}i\text{-}Pr)_3$ (180 μL) was added, and the resulting solution was heated at 90 °C for 1 h. After standing overnight, the solution was evaporated to dryness and the residue was applied as a dichloromethane solution to silica gel preparative TLC plates. Elution with dichloromethane gave three bands. Extraction of the purple third band with ethyl acetate gave 260 mg of a mixture containing the desired product. A second TLC

(3) Wang, R.; Sun, S.; Bekos, E. J.; Bright, F. V. *Anal. Chem.* **1995**, *67*, 149.
(4) Demas, J. N.; Crosby, G. A. *J. Phys. Chem.* **1971**, *75*, 991.
(5) Parker, C. A.; Rees, W. T. *Analyst* **1962**, *87*, 83.
(6) Mills, A.; Lepre, A. *Anal. Chem.* **1997**, *69*, 4653.
(7) Yappert, M. C.; Ingle, J. D. *Appl. Spectrosc.* **1989**, *43*, 759.
(8) Tucker, S. A.; Amszi, V. L.; Acree, W. E., Jr. *J. Chem. Educ.* **1992**, *69*, A11.
(9) Heitz, M. P.; Bright, F. V. *Appl. Spectrosc.* **1995**, *49*, 20.
(10) Bright, F. V. *Appl. Spectrosc.* **1995**, *49*, 14A.
(11) Barltrop, J. A.; Coyle, J. D. *Principles of Photochemistry*, John Wiley & Sons: New York, 1978.

separation using ca. 2% ethyl acetate in dichloromethane gave 39 mg, 10%, of $Ru(CO)_2(P(O\text{-}i\text{-}Pr)_3)_2$(AL-2H) by extraction of the beet red third band: IR (CH_2Cl_2) 2062.3 s, 2000.3 s cm^{-1}; ^1H NMR ($CDCl_3$) 8.21 (t, $J = 8$ Hz, 2 H), 8.76 (m, 3 H), 6.61 (d, $J = 8$ Hz, 1 H), 4.80 (sept, $J = 6$ Hz, 12 H), 1.23 (dd, $J_{HH} = 6$ Hz, $J_{PH} = 28$ Hz, 36 H) ppm; $^{31}P\{^1H\}$ NMR ($CDCl_3$) 110.7 (s) ppm.

(e) $Ru(CO)_2(TPPTS)_2$(AL-2H). A solution of $Ru_3(CO)_{12}$ (35 mg, 55 μmol), TPPTS (204 mg, ca. 324 μmol), and alizarin (43 mg, 179 μmol) in DMSO (15 mL) was heated at 80 °C under an argon atmosphere for 8 h. Then the atmosphere was changed to CO and the solution was heated at 90 °C for 2.5 h. The resulting solution was evaporated on a rotavap, and the purple residue was dissolved in methanol. This solution was filtered, and the filtrate was then treated with 2-propanol to yield a purple solid, 212 mg, contaminated with 16% OTPPS, as evidenced by the ^{31}P NMR spectrum. Characterization: IR (H_2O): 2060.0 s, 2002.8 s cm^{-1}; ^1H NMR (D_2O) 8.07 (br d, $J = 8$ Hz, 1 H), 7.97 (m, 11 H), 7.69 (br d, $J = 8$ Hz, 12 H), 7.63 (m, 1 H), 7.51 (m, ca. 15 H), 6.86 (d, $J = 8$ Hz, 1 H), 6.00 (d, $J = 8$ Hz, 1 H) ppm; $^{31}P\{^1H\}$ NMR (D_2O) 35.5 (s, 16%, OTPPS), 25.3 (s, 84%) ppm.

(f) $Ru(CO)(dppe)(PBu_3)$(AL-2H). A solution of $Ru_3(CO)_{12}$ (103.1 mg, 161 μmol), dppe (194.6 mg, 489 μmol), and alizarin (125.3 mg, 522 μmol) in toluene (25 mL) was heated at reflux under an argon atmosphere for 4 h. Then PBu_3 (120 μL, 481 μmol) was added, and refluxing was continued for 6 h. The resulting solution was evaporated to dryness and the residue was recrystallized from dichloromethane/methanol: yield 370 mg, 79%; IR (CH_2Cl_2) 1942.7 s cm^{-1}; ^1H NMR ($CDCl_3$) 8.97 (dd, $J = 8$, 10 Hz, 2 H), 8.38 (d, $J = 7.6$ Hz, 1 H), 8.20 (d, $J = 7.2$ Hz, 1 H), 8.07 (m, 2 H), 7.85 (br t, $J = 7$ Hz, 2 H), 7.68 (t, $J = 7.2$ Hz, 1H), 7.6−7.4 (m, 10 H), 7.37 (d, $J = 8.4$ Hz, 1 H), 6.91 (dd, $J = 7.2$, 10.8 Hz, 2 H), 6.66 (td, $J = 7.6$, 1.6 Hz, 2 H), 6.60 (dd, $J = 6.4$, 1.6 Hz, 1 H), 6.40 (d, $J = 8.0$ Hz, 1 H), 3.01 (dm, $J_{PH} = 41$ Hz, 1 H), 2.61 (dm, $J_{PH} = 39$ Hz, 1 H), 2.42 (m, 1 H), 2.03 (m, 1 H), 1.27 (m, 6 H), 1.14 (m, 6 H), 1.06 (m, 6 H), 0.69 (t, $J = 7.2$ Hz, 9 H) ppm; $^{31}P\{^1H\}$ NMR ($CDCl_3$) 59.7 (dd, 1 P_a), 43.4 (dd, 1 P_b), 17.9 (dd, 1 P_c) ppm, $J_{ab} = 12$ Hz, $J_{ac} = 23$ Hz, $J_{bc} = 350$ Hz. Anal. Calcd for $C_{53}H_{57}O_5P_3Ru$: C, 65.76; H, 5.94. Found: C, 65.55; H, 5.95.

(g) $Ru(CO)_2(PBu_3)_2$(AR-2H). A solution of $Ru_3(CO)_{12}$ (97 mg, 150 μmol), PBu_3 (240 μL, 960 μmol), and anthrarobin (Aldrich technical grade, 85% purity, 105 mg, 465 μmol) in toluene (30 mL) was heated at reflux under an argon atmosphere for 14 h. The resulting solution was evaporated to dryness, and the residue was applied as a dichloromethane solution to a silica gel preparative TLC plate. Elution with first dichloromethane and then 6% acetone in dichloromethane gave red, beet red, orange, purple, purple, and yellow bands, in order of decreasing R_f. Extraction of the yellow band with ethyl acetate gave 135 mg (172 μmol, 38%) of a material whose IR and NMR data were identical to those of the yellow product from alizarin. Extraction of the beet red band gave 87.3 mg of $Ru(CO)_2(PBu_3)_2$(AL-2H), (109 μmol, 24%); this product was presumed to arise from alizarin impurity in the starting material.

(h) $RuH(CO)(PPh_3)_2$(AL-H). A solution of $RuH_2(CO)(PPh_3)_3$ (175 mg, 191 μmol) and alizarin (58 mg, 242 μmol) in 2-methoxyethanol (10 mL) was heated at reflux under an argon atmosphere for 30 min. The resulting dark solution was evaporated to dryness, and the residue was applied as a dichloromethane solution to a silica gel preparative TLC plate. Elution with dichloromethane gave one green, and two purple bands. Extraction of the green top band with ethyl acetate and recrystallization from dichloromethane/methanol gave the product as green crystals. Yield: 108 mg, 63%.

(i) $RuH(CO)(PPh_3)_2$(QN-H) and $RuH(CO)(PPh)_2$(LQN-H). A solution of $RuH_2(CO)(PPh_3)_3$ (196 mg, 214 μmol) and quinizarin (52 mg, 217 μmol) in 2-methoxyethanol (10 mL) was heated at reflux under an argon atmosphere for 30 min. The resulting green solution was evaporated to dryness, and the residue was applied as a dichloromethane solution to silica gel preparative TLC plates. Elution with 1:1 dichloromethane/hexanes gave a yellow, a green, and another yellow band. The green band was extracted with ethyl acetate; evaporation gave $RuH(CO)(PPh_3)_2$(QN-H) (96 mg, 49%). Recrystallization from dichloromethane/methanol gave green crystals. Extraction of the yellow third band gave $RuH(CO)(PPh_3)_2$(LQN-H) (71 mg, 36%).

$RuH(CO)(PPh_3)_2$(QN-H): IR (CH_2Cl_2) 1915 cm^{-1}; ^1H NMR ($CDCl_3$) 14.06 (s, 1 H), 8.14 (d, $J = 8$ Hz, 1 H), 8.05 (d, $J = 8$ Hz, 1 H), 7.58 (m, 14 H), 7.18 (m, 20 H), 6.61 (d, $J = 9.2$ Hz, 1 H), 6.31 (d, $J = 9.2$ Hz, 1 H), −13.92 (t, $J = 20$ Hz, 1 H) ppm, minor isomer hydride at −13.83 (t, $J = 19$ Hz) ppm, major/minor ∼12; $^{31}P\{^1H\}$ NMR ($CDCl_3$) 43.6 (s) ppm.

$RuH(CO)(PPh_3)_2$(LQN-H): IR (CH_2Cl_2) 1915.8 cm^{-1}; ^1H NMR ($CDCl_3$) 14.06 (s, 1H), 8.14 (d, $J = 8$ Hz, 1 H), 7.94 (d, $J = 8$ Hz, 1 H), 7.62 (m, 13 H), 7.38 (t, $J = 7.4$ Hz, 1 H), 7.2 (m, 18 H), 2.29 (t, $J = 7$ Hz, 2 H), 2.16 (t, $J = 7$ Hz, 2 H), −13.84 (t, $J = 20$ Hz, 1 H); $^{31}P\{^1H\}$ NMR ($CDCl_3$) 43.6 (s) ppm.

(j) $[Ru(CO)_2(PPh_3)_2$(AL-2H)]$SbCl_6$, $[Ru(CO)_2(PCyc_3)_2$(AL-2H)]-$SbCl_6$, and $[Ru(CO)_2(PBu_3)_2$(AR-2H)]$SbCl_6$. Semiquinone complexes were prepared by adding a stoichiometric amount of tris(4-bromophenyl)ammoniumyl hexachloroantimonate (Aldrich) to a dichloromethane solution of the appropriate complex. IR and EPR spectra were then immediately recorded. The semiquinone complexes decomposed within a few hours. IR (CH_2Cl_2): $[Ru(CO)_2(PPh_3)_2$(AL-2H)]-$SbCl_6$, 2071.3 s, 2019.5 m cm^{-1}; $[Ru(CO)_2(PCyc_3)_2$(AL-2H)]$SbCl_6$, 2055.9 vs, 2001.6 s cm^{-1}; $[Ru(CO)_2(PBu_3)_2$(AR-2H)]$SbCl_6$, 2057.9 vs, 2000.3 s cm^{-1}.

(k) $[Ru(CO)(dppe)(PBu_3)$(AL-2H)]PF_6. Ferrocenium hexafluorophosphate (36 mg) was added as a dichloromethane suspension to a solution of $Ru(CO)(dppe)(PBu_3)$(AL-2H) (103 mg) in dichloromethane (20 mL). After 20 min, the IR spectrum indicated complete reaction. The solution was reduced in volume on a rotavap, followed by the addition of hexanes. The purple solution was pipetted off, and remaining purple solid was washed with hexanes and dried. Yield: 43 mg, 36%. Subsequent crops were contaminated with starting material. IR (CH_2Cl_2) 1976.6 cm^{-1}. Anal. Calcd for $C_{53}H_{57}O_5F_6P_4Ru$: C, 57.20; H, 5.16. Found: C, 55.20; H, 5.16. Ion exchange with sodium tetraphenylborate and recrystallization from dichloromethane/toluene gave a small amount of $[Ru(CO)(dppe)(PBu_3)$(AL-2H)]BPh_4. Anal. Calcd for $C_{77}H_{77}O_5BP_3Ru$: C, 71.85; H, 6.03. Found: C, 71.17; H, 6.36.

Crystal Structure Analysis of *trans*-$RuH(CO)(PPh_3)_2$(AL-H). The crystal chosen for the analysis, a well-formed red parallelepiped of dimensions 0.2 × 0.25 × 0.65 mm, was sealed in a thin-walled glass capillary and mounted on a Siemens R3m/V diffractometer. Cell constants were derived from a least-squares fit of 50 carefully centered reflections with 2θ(Mo Kα) = 25−30°, which were well dispersed throughout reciprocal space. Data were collected as described previously[12] and were corrected for Lorentz and polarization effects and for absorption.

All calculations were performed under the SHELXTL PLUS (Release 4.11 VMS) program package.[13] The analytical scattering factors for neutral atoms[14a] were corrected for anomalous dispersion.[14b] The structure was solved by direct methods and difference Fourier techniques and refined by least-squares procedures. All non-hydrogen atoms were refined anisotropically. All organic hydrogen atoms were included in optimized positions with d(C−H) = 0.96 Å.[15] Atoms H(1) (the hydride ligand) and H(2) (bonded to O(2) in the AL-H ligand) were located on a difference Fourier map, and their positions were refined. Data for the crystallographic study are collected in Table 1.

Results and Discussion

The coordination chemistry of hydroxyanthraquinones has not received much recent attention. Although complexes of alizarin have been used for centuries as dyes, structural information appears to be slight. A search of the Cambridge Structural Database found only three references containing crystal structures, all of coordination complexes involving bridging between

(12) Churchill, M. R.; Lashewycz, R. A.; Rotella, F. J. *Inorg. Chem.*, **1977**, *16*, 265.
(13) Sheldrick, G. M. *SHELXTL PLUS (Release 4.11 VMS)*; Siemens Analytical Instruments Inc.; Madison, WI, 1990. (See also Siemens SHELXTL PLUS Manual, 2nd ed., 1990).
(14) International Tables for X-ray Crystallography; Kynoch Press: Birmingham, England, 1974; Vol. 4 (a) pp 99−101, (b) pp 149−150.
(15) Churchill, M. R. *Inorg. Chem.*, **1973**, *12*, 1213.

Scheme 1

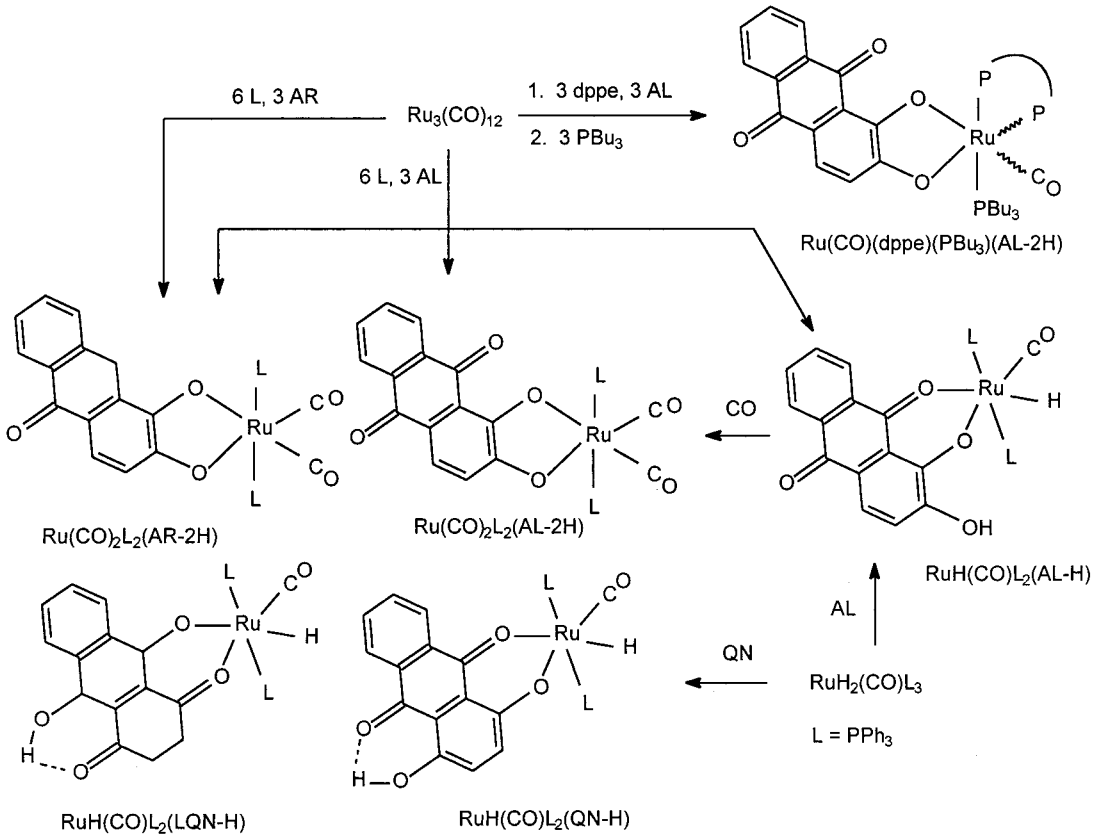

Table 1. Crystal Data for $RuH(CO)(PPh_3)_2$((AL-H)

empirical formula	$C_{51}H_{38}O_5P_2Ru$
fw	893.8
wavelength, Å	0.710 730
crystal system	monoclinic
space group	*C*2/*c* (No. 15)
a, Å	32.862(8)
b, Å	13.377(3)
c, Å	22.841(6)
β, deg	124.39(2)
V, Å^3	8285(4)
Z	8
d_{calcd}, Mg/m^3	1.433
F(000)	3664
μ, mm^{-1}	0.493
2θ range, deg	5.0−45.0
no. of reflns collected	5842
no. of unique reflns	5442 (R_{int} = 1.08%)
no. of reflns >2σ(*I*)	3829
abs. corr	ψ scans
max and min transm	0.9584 and 0.9360
final *R* indices [*I* > 2σ(*I*)]	R1 = 3.74%, wR2 = 3.38%
R indices (all data)	R1 = 6.52%, wR2 = 3.77%
largest diff peak and hole, (e/Å^3)	0.36, −0.27

two metals.[16] The bridged complexes $Ca_2Al_2(OH)_2(AL\text{-}2H)_4$, its purpurin analogue, and $Ca_2Ti_2O_2(AL\text{-}2H)_4$ contain 1,2-coordination to Al or Ti and 1,9-coordination to Ca.[16a] A number of studies on coordination complexes of dihydroxyanthraquinones and related ligands have appeared, most suggesting 1,9-coordination.[17−22] The most complete studies have concerned complexes of $[Ru^{II}(bpy)_2]$. A Ru complex of alizarin has been shown to undergo interconversion between 1,2- and 1,9-chelating forms, induced by deprotonation.[22] Dimetallic 1,9-quinizarin coordination complexes of Fe have been crystallographically characterized, as well as a dimetallic complex derived from 5,8-dihydroxynaphthoquinone.[16b,c]

Reactions of $Ru_3(CO)_{12}$ with alizarin and phosphine ligands L = PBu_3, $PCyc_3$, and PPh_3 in refluxing toluene give as the major products $RuH(CO)L_2$(AL-H), $Ru(CO)_2L_2$(AL-2H), and $Ru(CO)_2L_2$(AR-2H), with the relative amounts depending upon L and the reaction time (see Scheme 1); the analogous reaction with L = P(*m*-$NaSO_3C_6H_4)_3$ (TPPTS) in DMSO gives $Ru(CO)_2$-$(TPPS)_2$(AL-2H). The reaction most likely proceeds by oxidative addition of the catechol, which serves as the hydrogen source for reduction of the quinone, with $RuH(CO)L_2$(AL-H) as an intermediate complex. Consistent with this, $RuH(CO)(PPh_3)_2$-(AL-H) reacts with CO in refluxing toluene to give $Ru(CO)_2$-$(PPh_3)_2$(AL-2H) within 1 h. However, $Ru(CO)_2(PPh_3)_2$(AL-2H) does not form $RuH(CO)(PPh_3)_2$(AL-H) under a hydrogen atmosphere.

Under similar conditions, the reactions of alizarin, $Ru_3(CO)_{12}$, and L = $P(OPh)_3$ and P(O-*i*-Pr)$_3$ did not give the analogous products. A low yield of $Ru(CO)_2$(P(O-*i*-$Pr_3)_2$(AL-2H) was

(16) (a) Wunderlich, C.-H.; Bergerhoff, G. *Chem. Ber.* **1994**, *127*, 1185. (b) Pierpont, C. G.; Francesconi, L. C.; Hendrickson, D. N. *Inorg. Chem.* **1978**, *17*, 3470. (c) Maroney, M. J.; Day, R. O.; Psyris, T.; Fleury, L. M.; Whitehead, J. P. *Inorg. Chem.* **1989**, *28*, 173.
(17) Masoud, M. S.; Tawfik, M. S.; Zayan, S. E. *Synth. React. Inorg. Met.-Org. Chem.* **1984**, *14*, 1
(18) Bulatov, A. V.; Khidekel, M. L.; Egorochkin, A. N.; Panicheva, M. V.; Sennikov, P. G. *Transition Met. Chem.* **1983**, *8*, 289.
(19) (a) Gooden, V. M.; Cai, H.; Dasgupta, T. P.; Gordon, N. R.; Hughes, L. J.; Sadler, G. G. *Inorg. Chim. Acta* **1997**, *255*, 105. (b) Merrell, P. H. *Inorg. Chim. Acta* **1979**, *32*, 99.
(20) Dei, A.; Gatteschi, D.; Pardi, L. *Inorg. Chem.* **1990**, *29*, 1442.
(21) (a) Tsipis, C. A.; Bakalbassis, E. G.; Papageorgiou, V. P.; Bakola-Christianopoulou, M. N. *Can. J. Chem.* **1982**, *60*, 2477. (b) Bakola-Christianopoulou, M. N. *Polyhedron* **1984**, *3*, 729.
(22) DelMedico, A.; Auburn, P. R.; Dodsworth, E. S.; Lever, A. B. P.; Pietro, W. J. *Inorg. Chem.* **1994**, *33*, 1583.

obtained by first refluxing $Ru_3(CO)_{12}$ and alizarin in toluene, followed by treatment with $P(O\text{-}i\text{-}Pr)_3$.

1,2-Catecholate Complexes. Characterizations of $Ru(CO)_2L_2$-(AL-2H) are straightforward by comparison to those of previously reported catecholate complexes. The observation of two CO stretches in the IR spectra and a single ^{31}P resonance for each complex indicate that all are $Ru(cis\text{-}CO)_2(trans\text{-}PR_3)_2$-(chelating ligand) complexes. The ^1H NMR spectra show no O−H resonances, and the expected six aromatic proton resonances can be observed for the PBu_3 and $PCyc_3$ complexes, although the aromatic region is largely obscured for the PPh_3 complex. The AL-2H complexes each show a pair of doublets for the 3- and 4-hydrogens, which because of the upfield shift of the 3-hydrogen resonance (at ca. 6.5 ppm) are useful for characterization. For complexes with Ph-substituted phosphines, ring current effects shift the 3-hydrogen resonance upfield still further to ca. 6.0 ppm. The complex $Ru(CO)_2(PBu_3)_2$(AR-2H) can be prepared in higher yield by the analogous reaction with anthrarobin, thus confirming the 9,9-dihydro structure.

The product formed from dppe was too insoluble to allow for facile characterization, so further substitution using PBu_3 was performed. Ru(CO)(dppe)(PBu_3)(AL-2H) is a very soluble, deep blue compound. Its ^{31}P NMR spectrum indicates predominantly one isomer with PBu_3 occupying one site cis to the alizarinate chelate and one end of the dppe ligand occupying the other. The large trans P−P coupling constant of 350 Hz, compared with the small cis values of 12 and 23 Hz, is diagnostic.

The complexes are highly stable to heat and air. Most are quite soluble in dichloromethane, and the PBu_3 complex is soluble in hydrocarbons. In contrast, the TPPTS complex is very soluble in water and soluble in methanol or DMSO but insoluble in dichloromethane. The complexes do not react with carboxylic acids under mild conditions but release alizarin in the presence of a large excess and at elevated temperatures. Strong acids such as CF_3CO_2H rapidly cause generation of alizarin.

The presence of the 9,10-dioxo substituents suggested that these complexes might show significant hydrogen bonding. Direct evidence for such hydrogen bonding comes from the CO stretching frequencies; addition of butanol to a solution of $Ru(CO)_2(PBu_3)_2$(AL-2H) in hexanes results in the appearance of a set of two absorbances at 2038 and 1970 cm^{-1}, attributed to the hydrogen-bonded complex, in addition to absorbances at 2030 and 1965 cm^{-1}, due to the free complex. However, this hydrogen bonding is not associated with the 9,10-dioxo substituents, since similar shifts are observed for the analogous catecholate, $Ru(CO)_2(PBu_3)_2(O_2C_6H_4)$.

1,9-Complexes. Reactions of $Ru_3(CO)_{12}$, PR_3 (R = Ph, Cyc), and alizarin in the 1:6:3 ratios in refluxing toluene generate $RuH(CO)(PR_3)_2$(AL-H), in addition to $Ru(CO)_2(PR_3)_2$(AL-2H). The former product is exclusively formed from $H_2Ru(CO)$-$(PPh_3)_3$ and alizarin in refluxing 2-methoxyethanol, and the analogous reaction with quinizarin gives $RuH(CO)(PR_3)_2$(QN-H) and $RuH(CO)(PR_3)_2$(LQN-H). The singlet ^{31}P signal indicates a trans arrangement of PR_3 ligands. The ^1H NMR and IR spectra are similar to those of $RuH(CO)(PPh_3)_2$(acac).[23] The ^1H NMR spectra of the AL-H complexes contain an HO resonance at ca. 7−7.5 ppm and the 3-hydrogen resonance is not shifted as far upfield as it is for the 1,2-complexes $Ru(CO)_2L_2$(AL-2H). Two isomers due to the relative orientations of the *cis*-(H)(CO) ligands are expected, but one predominates by >10:1. The structure of what we assume to be the predominant isomer was confirmed by a single-crystal X-ray diffraction study for $RuH(CO)(PPh_3)_2$(AL-H). On electronic grounds, one would expect the stronger σ donor phenoxide to favor the position trans to the strong π acceptor CO rather than the strong σ donor hydride, as is observed.

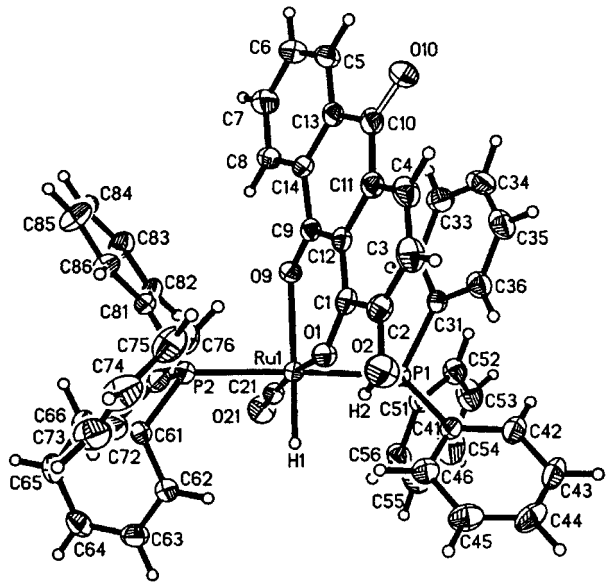

Figure 1. Molecular geometry of the $RuH(CO)(PPh_3)_2$(AL-H) molecule.

Table 2. Selected Bond Lengths (Å) and Angles for $RuH(CO)(PPh_3)_2$((AL-H)

(A) Ruthenium−Ligand Bond Lengths			
Ru−H(1)	1.56(4)	Ru−O(1)	2.119(4)
Ru−P(1)	2.367(1)	Ru−O(9)	2.180(4)
Ru−P(2)	2.372(2)	Ru−C(21)	1.789(7)
(B) Distances within the Alizarin System			
C(1)−O(1)	1.308(8)	C(7)−C(8)	1.375(7)
C(1)−C(2)	1.418(7)	C(8)−C(14)	1.387(7)
C(1)−C(12)	1.410(7)	C(9)−O(9)	1.250(8)
C(2)−O(2)	1.349(7)	C(9)−C(12)	1.447(6)
C(2)−C(3)	1.361(11)	C(9)−C(14)	1.483(7)
C(3)−C(4)	1.389(9)	C(10)−O(10)	1.227(10)
C(4)−C(11)	1.370(7)	C(10)−C(11)	1.467(8)
C(5)−C(6)	1.373(8)	C(10)−C(13)	1.471(8)
C(5)−C(13)	1.390(8)	C(11)−C(12)	1.444(10)
C(6)−C(7)	1.376(12)	C(13)−C(14)	1.413(11)
(C) Angles around the Ruthenium(II) Center			
H(1)−Ru−P(1)	88.7(15)	P(1)−Ru−C(21)	91.7(2)
H(1)−Ru−P(2)	88.8(15)	P(2)−Ru−O(1)	94.5(1)
H(1)−Ru−O(1)	91.9(16)	P(2)−Ru−O(9)	88.8(1)
H(1)−Ru−O(9)	173.5(15)	P(2)−Ru−C(21)	88.0(2)
H(1)−Ru−C(21)	81.6(16)	O(1)−Ru−O(9)	82.3(1)
P(1)−Ru−P(2)	177.5(1)	O(1)−Ru−C(21)	173.0(2)
P(1)−Ru−O(1)	85.5(1)	O(9)−Ru−C(21)	104.3(2)
P(1)−Ru−O(9)	93.7(1)		

Description of the Molecular Structure for $RuH(CO)(PPh_3)_2$(AL-H). Figure 1 shows the molecular structure and labeling scheme, and selected bond lengths and angles are provided in Table 2. The central ruthenium(II) moiety has a fairly regular octahedral coordination sphere with trans PPh_3 ligands (Ru−P(1) = 2.367(1) Å and Ru−P(2) = 2.372(2) Å) and mutually cis hydride (Ru−H(1) = 1.56(4) Å) and carbonyl (Ru−C(21) = 1.789(7) Å) ligands. The alizarin system is linked to ruthenium via atoms O(1) and O(9), with Ru(1)−O(1) = 2.119(4) Å (trans to the carbonyl ligand) and Ru−O(9) = 2.180(4) Å (trans to the hydride ligand). The C−O distances in the chelate ring are C(1)−O(1) = 1.308(8) Å and C(9)−O(9) = 1.250(8) Å, as compared to values of C(2)−O(2) =

(23) Queiros, M. A. M.; Robinson, S. D. *Inorg. Chem.* **1978**, *17*, 310.

1.349(7) Å (for the C(sp^2)−OH single bond) and C(10)−O(10) = 1.227(10) Å (for the C═O double bond) associated with the uncoordinated oxygen atoms.

The isomer identified should be preferred on electronic grounds. The π acceptor CO ligand is oriented trans to the stronger σ donor phenoxy end of the chelate while the stronger σ donor hydride is trans to the π acceptor keto end.

The crystal structure as a whole is stabilized by a series of C−H···O hydrogen bonds and by the parallel stacking of alizarin-H systems (see Figure 1S, Supporting Information). The six-membered chelate ring is nonplanar, with a dihedral angle of 13.6° between the O(1)−Ru−O(9) and C(1)−C(12)−C(9) moieties. The nonplanarity is due to π stacking of the alizarinate ring between a phenyl group (C(31)−C(36)) attached to P(1) in the same molecule and on an adjacent molecule in the crystal. The polycyclic aromatic system is closer to planarity with a dihedral angle of only 6.0° between the two outermost six-membered rings (viz., C(1)−C(2)−C(3)−C(11)−C(12) and C(5)−C(6)−C(7)−C(8)−C(14)−C(13) in Figure 1).

A search of the Cambridge Structure Database found no other examples of monometallic 1,9-alizarinate complexes, but there are structures for $Ca_2Al_2(OH)_2(AL\text{-}2H)_4(H_2O)_5(DMF)_7$ and $Ca_2Ti_2O_2(AL\text{-}2H)_4(H_2O)_5(DMF)_5$.[16a] In these structures, the alizarinate dianion forms a 1,9-chelate with the calcium ion and a 1,2-chelate with the other metal ion. In comparison with these structures, there is a significant difference between the two sets of phenolic C-bond lengths, as well as a notably longer C(9)−O(9) bond. Another related structure is that of $\{Fe(salen)\}_2(QN\text{-}2H)$, in which the quinizarinate dianion bridges the two Fe ions, forming a 1,9:4,10-chelate.[16b]

Electrochemistry. An electrochemical study of $Ru(bpy)_2(1,2\text{-}AL\text{-}2H)$ and $[Ru(bpy)_2(AL\text{-}H)]^+$ was reported previously.[22] The cyclic voltammogram (CV) of $Ru(bpy)_2(1,2\text{-}AL\text{-}2H)$ displays two reversible 1-e oxidations at +0.06 and +0.88 V (acetonitrile) vs SCE (−0.36 and +0.46 V vs ferrocene) and irreversible reductions at −1.58 and −1.70 V for the *p*-quinone/*p*-semiquinone and *p*-semiquinone/hydroquinonate couples.

The electrochemistry of these complexes was surveyed using cyclic voltammetry. Representative CVs are shown in Figure 2 ((a) $Ru(CO)_2(PPh_3)_2(AL\text{-}2H)$ and (b) $Ru(CO)_2(PCyc_3)_2(AL\text{-}2H)$) and Figure 3 ((a) $RuH(CO)(PPh_3)_2(AL\text{-}H)$ and (b) $RuH(CO)(PCyc_3)_2(AL\text{-}H)$). Electrochemical data are summarized in Table 3.

In the most favorable case, the 1,2-catecholate complexes could exhibit two 1-e oxidations associated with the catecholate moiety and several 1-e reductions associated with the central quinone. All of the 1,2-catecholates exhibit a reversible to quasi-reversible 1-e oxidation, at potentials of −0.09 to +0.18 V. The oxidation potential is not very sensitive to the other ligands in the complex, as expected for a ligand-centered process. The CO stretching frequencies are excellent indicators of the electron densities on the metal centers and correlate well with metal-centered Ru(II)/Ru(III) oxidation potentials. The dependence of Ru(II)/Ru(III) oxidation potentials upon the ligands has been parametrized by Lever,[24] allowing a quantitative prediction of differences in these oxidation potentials for the various complexes. There is a poor correlation of the oxidation potentials for $Ru(CO)_2L_2(AL\text{-}2H)$, although the lowest oxidation potential is associated with the most electron-rich metal center: that of $Ru(CO)(dppe)(PBu_3)(AL\text{-}2H)$. If the 1-e oxidation were metal centered, one would have expected the oxidation potential for $Ru(CO)_2(PBu_3)_2(AL\text{-}2H)$ to be ca. 0.2 V lower than that for

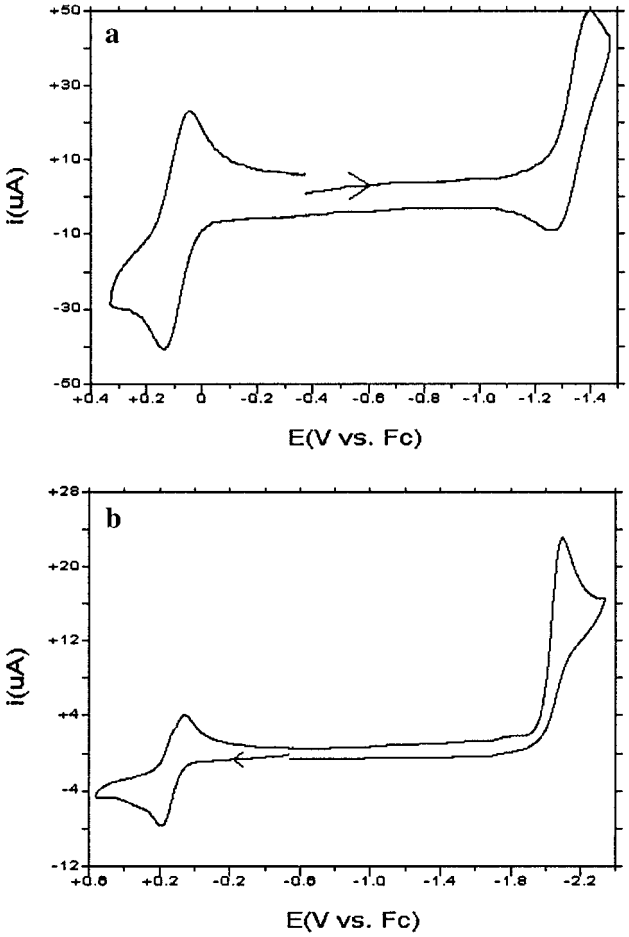

Figure 2. Cyclic voltammograms for (a) $Ru(CO)_2(PPh_3)_2(AL\text{-}2H)$ and (b) $Ru(CO)_2(PCyc_3)_2(AL\text{-}2H)$.

$Ru(CO)_2(PPh_3)_2(AL\text{-}2H)$; instead, its oxidation potential is higher by 0.07 V. Furthermore, the oxidation potential for $Ru(CO)_2(PBu_3)_2(AL\text{-}2H)$ would have been expected to be ca. 0.6 V higher than that of $Ru(CO)(dppe)(PBu_3)(AL\text{-}2H)$; instead, its potential is only 0.27 V more positive. With only one example having a non-carbonyl ligand trans to the alizarinate ring, it is impossible to rule out a stronger trans influence upon the oxidation potential, but clearly there is little, if any, influence due to the cis PR_3 ligands, inconsistent with a metal-centered redox process. On the other hand, the oxidation potential is strongly dependent upon the catecholate ring; the alizarinate complex $Ru(CO)_2(PBu_3)_2(AL\text{-}2H)$ (+0.18 V) displays a much more positive oxidation potential than $Ru(CO)_2(PBu_3)_2(AR\text{-}2H)$ (−0.056 V) and $Ru(CO)_2(PBu_3)_2(Cat)$ (−0.248 V), which have the less electron-withdrawing ring substituents. In fact, there is a strong correlation between these oxidation potentials and the Hammett parameters[25] for the $C_6R_4O_2$ substituents, consistent with a ligand-centered redox process. The second 1-e oxidation is only accessible for complexes with stronger electron-donating ligands. The oxidative electrochemistry of $Ru(CO)_2(PBu_3)_2(AL\text{-}2H)$ is similar to the responses of other $Ru(CO)_2L_2(Cat)$ complexes previously reported.[26] The CV recorded at 100 mV/s in a 0.1 M TBATFB/dichloromethane solution displays a reversible 1-e oxidation at +0.2 V vs Fc and a quasi-reversible

(24) Lever, A. B. P. *Inorg. Chem.* **1990**, *29*, 1271.

(25) Hansch, C.; Leo, A.; Taft, R. W. *Chem. Rev.* **1991**, *91*, 165.

(26) (a) Connelly, N. G.; Manners, I.; Protheroe, J. R. C.; Whiteley, M. W. *J. Chem. Soc., Dalton Trans.* **1984**, 2713. (b) Bohle, D. S.; Goodson, P. A. *J. Chem. Soc., Chem. Commun.*, **1992**, 1205. (c) Bohle, D. S.; Carron, K. T.; Christensen, A. N.; Goodson, P. A.; Powell, A. K. *Organometallics* **1994**, *13*, 1355.

Table 3. Cyclic Voltammetric Data

complex	$(E_{p,a} + E_{p,c})/2$ $[E_{p,a}]$, (V)	ΔE_p (mV)	i_{pc}/i_{pa}	$(E_{p,a} + E_{p,c})/2$ $[E_{p,c}]$, (V)	ΔE_p (mV)	i_{pa}/i_{pc}
$Ru(CO)_2(PPh_3)_2$(AL-2H) (400 mV/s)	+0.11	81	0.98	−1.34	136	0.69
$Ru(CO)_2(PBu_3)_2$(AL-2H) (800 mV/s)	+0.18	80	1.0	−1.95	102	0.79
Ru(CO)(dppe)(PBu_3)(AL-2H) (100 mV/s)	−0.09	88	1.0			
$Ru(CO)_2(PCyc_3)_2$(AL-2H) (100 mV/s)	+0.13	78	0.66	[−2.05]		
				3-e process		
$Ru(CO)_2(PBu_3)_2$(AR-2H) (100 mV/s)	−0.056	80	0.57			
$RuH(CO)(PPh_3)_2$(AL-H) (100 mV/s)	[+0.41]			−1.64	86	
$RuH(CO)(PCyc_3)_2$(AL-H) (100 mV/s)	+0.076	58		−1.40	62	
				−1.67	67	
$Ru(CO)_2(TPPTS)_2$(AL-2H) (100 mV/s)	+0.14	78	0.9	[−1.8]		

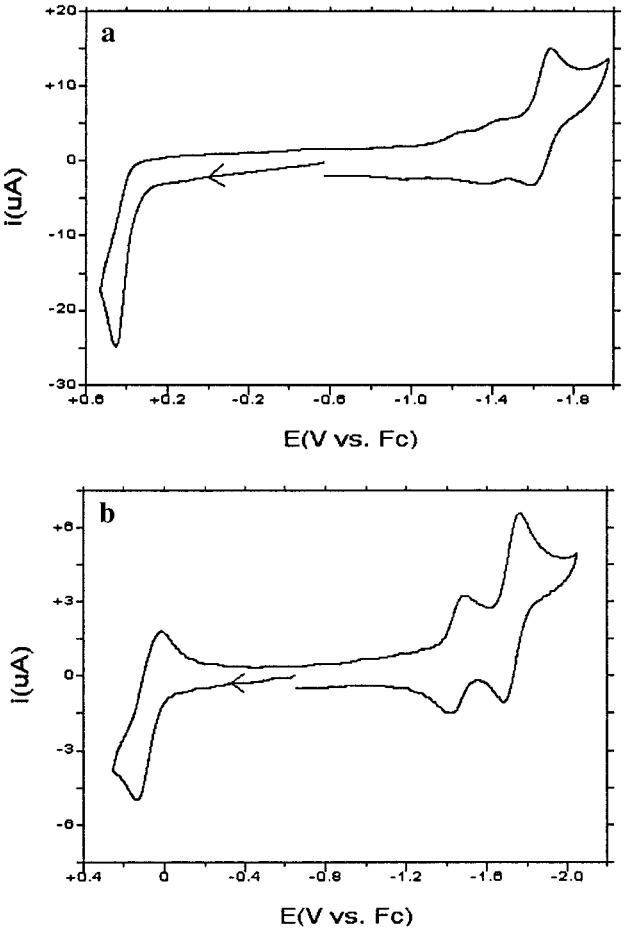

Figure 3. Cyclic voltammograms for (a) $RuH(CO)(PPh_3)_2$(AL-H) and (b) $RuH(CO)(PCyc_3)_2$(AL-H).

1-e oxidation at ca. +1.05 V. For comparison, $Ru(CO)_2(PPh_3)_2$-(*o*-$O_2C_6Cl_4$) displays reversible 1-e oxidations at 0.58 and 1.58 V vs SCE (ca. 0.16 and 1.16 V vs ferrocene). Consistent with other studies, both oxidations are presumed to be ligand-based. The reduction processes are much more variable.

The two examples of $RuH(CO)(PR_3)_2$(AL-H) display very different electrochemical behaviors. Figure 3 shows the CVs for (a) $RuH(CO)(PPh_3)_2$(AL-H) and (b) $RuH(CO)(PCyc_3)_2$(AL-H). The 1-e oxidation of $RuH(CO)(PPh_3)_2$(AL-H) is completely irreversible up to 800 mV/s ($E_{p,a}$ = +0.41 V at 100 mV/s), whereas $RuH(CO)(PCyc_3)_2$(AL-H) displays a reversible 1-e oxidation at +0.076 V; on the basis of the Lever electrochemical parameters, the estimated oxidation potential for the former is 0.48 V for a metal-centered process and the latter should have an oxidation potential somewhat more than ca. 200 mV lower, comparable with the observed difference of less than 330 mV. Thus, it seems likely that the 1-e-oxidations in these complexes are primarily metal-centered. Unfortunately, the 1-e-oxidation products are too unstable for characterization. The reductions of these two complexes are also different. For $RuH(CO)(PPh_3)_2$-(AL-H), a single quasi-reversible 1-e reduction at −1.64 V is complicated by a prepeak, which we associate with adsorbed material. On the other hand, for $RuH(CO)(PCyc_3)_2$(AL-H), two quasi-reversible processes are found at −1.40 and −1.67 V. The similarities of the reduction potentials suggest that these are associated primarily with the anthracenedione units.

Semiquinone Complexes. Chemical oxidation was used to generate the semiquinone complexes $[Ru(CO)_2L_2(AL\text{-}2H)]^+$, $[Ru(CO)_2(PBu_3)_2(AR\text{-}2H)]^+$, and $[Ru(CO)(dppe)(PBu_3)_2(AL\text{-}2H)]^+$. The species $[Ru(CO)_2L_2(AL\text{-}2H)]^+$ (L = PBu_3, PPh_3, $PCyc_3$) and $[Ru(CO)_2(PBu_3)_2(AR\text{-}2H)]^+$ were prepared by oxidation with tris(4-bromophenyl)aminium hexachloroantimonate (magic blue) in dichloromethane solution. The IR spectra of the semiquinone complexes show that the CO stretches are shifted to higher frequency by ca. 20−30 cm^{-1} vs those of the neutral precursors. In each case, the IR spectrum decays over a period of hours to a second set of peaks (e.g., for L = PBu_3, IR bands at 2063.6 and 2009 cm^{-1} decay to carbonyl stretches at 2041 and 1975 cm^{-1}), attributed to the corresponding *cis*,*cis*,-*trans*-$RuCl_2(CO)_2L_2$ decomposition product, the chlorides coming from the hexachloroantimonate ion. At room temperature, the EPR spectra (Table 4) each display a strong signal near g = 2.00 with hyperfine couplings to two equivalent ^{31}P nuclei (t, $A(^{31}P) \approx 25$ G) and ^{99}Ru and ^{101}Ru (∼4 G for each), and, in most cases, also to two protons, assumed to be in the 3- and 4-positions. A representative EPR spectrum and a simulation, for $[Ru(CO)_2(PBu_3)_2(AL\text{-}2H)]^+$, are shown in Figure 4. The spectra are very similar to those of $[Ru(CO)_2(PPh_3)L(o\text{-}O_2C_6Cl_4)]^+$, reported by Connelly et al. (e.g., for L = PPh_3, g = 2.002 (t, $A(^{31}P)$ = 25.2 G).[26a]

For Ru(CO)(dppe)(PBu_3)(AL-2H), which has an oxidation potential less positive than that of ferrocene, $[FeCp_2]PF_6$ oxidation gives a relatively stable semiquinone complex, characterized by IR and EPR spectroscopy. The EPR spectrum (Table 4) is a broad triplet, indicating that the hyperfine coupling to the ^{31}P nucleus in the plane of the alizarinate ring is too small to resolve. The complex can be isolated as a solid (although not in analytically pure form) but decomposes within a few days in solution to regenerate Ru(CO)(dppe)(PBu_3)(AL-2H) and uncharacterized, non-carbonyl-containing material.

Photophysics. The color of alizarin−metal complexes was of primary interest to the dye industry around the turn of the last century.[2] Colors of the dyes ranged from red to brown. Recently, the structures and electronic absorption spectra of complexes of alizarin were reexamined.[16a] The absorption maximum was found to shift to shorter wavelengths with increasing electronegativity of the metal atom, varying from 432 nm for alizarin itself to 520 nm for the Al salt to 636 nm for the alizarinate dianion. The absorptions for the Al and Mg

Table 4. EPR Spectral Data from Dichloromethane Solutions

complex	g	$A(^{31}P)$, G	$A(^{1}H)$, G	$A(^{101}Ru, ^{99}Ru)$, G
$[Ru(CO)(dppe)(PBu_3)(AL\text{-}2H)]PF_6$	2.004	23.8 25.8 1.9	1.9 1.4	4.0 4.0
$[Ru(CO)_2(PBu_3)_2(AL\text{-}2H)]SbCl_6$	2.0056	26.4	2.30	4.0
$[Ru(CO)_2(PPh_3)_2(AL\text{-}2H)]SbCl_6$	2.0039	25.0	2.30	3.7, 3.9
$[Ru(CO)_2(PCyc_3)_2(AL\text{-}2H)]SbCl_6$	2.0058	25.3	2.3	4.6, 4.6
$[Ru(CO)_2(PBu_3)_2(AR\text{-}2H)]SbCl_6$	2.0052	24.11	1.80 (2H) 3.10 (1H)	

Table 5. UV/Vis Data between 350 and 820 nm

complex	λ_{max} (ϵ), nm
$HRu(CO)(PCyc_3)_2(AL\text{-}H)$[a]	486 (8.2×10^3), 600 br (1.7×10^3)
$HRu(CO)(PPh_3)_2(AL\text{-}H)$[a]	444 (6.2×10^3), 568 (2.7×10^3), 610 sh (2.1×10^3)
$Ru(CO)_2(PBu_3)_2(AL\text{-}2H)$[a]	552 (1.3×10^4)
$Ru(CO)_2(PCyc_3)_2(AL\text{-}2H)$[a]	360 (5.1×10^3), 526 sh (9.3×10^3), 558 (1.2×10^4), 600 sh (9.1×10^3)
$Ru(CO)_2(TPPTS)_2(AL\text{-}2H)$[b]	560 (9.2×10^3)
$Ru(CO)(dppe)(PBu_3)(AL\text{-}2H)$[a]	542 sh (9.3×10^3), 582 (1.2×10^4), 626 sh (9.0×10^3)
$Ru(CO)_2(PPh_3)_2(AL\text{-}2H)$[a]	554 (6.6×10^3)
$Ru(CO)_2(PBu_3)_2(AR\text{-}2H)$[a]	438 (8.8×10^3)
$[Ru(CO)(dppe)(PBu_3)(AL\text{-}2H)]PF_6$[a]	574 (4.0×10^3), 614 sh (3.5×10^3)
$HRu(CO)(PPh_3)_2(LQN\text{-}H)$[a]	358 (9.4×10^3), 468 (7.1×10^3), 494 (7.1×10^3)
$HRu(CO)(PPh_3)_2(QN\text{-}H)$[a]	356 (8.2×10^3), 468 (6.6×10^3), 494 sh (5.7×10^3), 648 br (1.8×10^3)

[a] In dichloromethane. [b] In water.

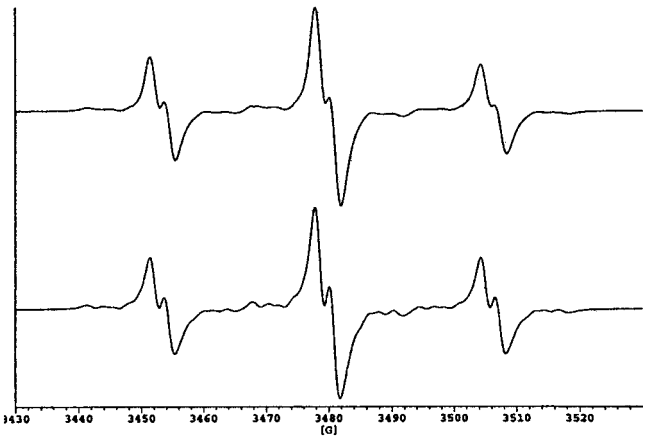

Figure 4. Experimental (upper) and simulated (lower) EPR spectra of $[Ru(CO)_2(PBu_3)_2(AL\text{-}2H)]^+$ in dichloromethane at room temperature.

complexes were each reported to exhibit significant charge transfer character to a MO with a strong metal contribution. The 1,2-complexes herein display absorptions at ca. 550 nm (dichloromethane solution) for violet $Ru(CO)_2L_2(AL\text{-}2H)$ and at 574 nm for the more electron-rich, dark blue $Ru(CO)(dppe)(PBu_3)(AL\text{-}2H)$. The 1,9-complexes are quite different, with absorption maxima at 444 nm for green $RuH(CO)(PPh_3)_2(AL\text{-}H)$ and at 486 nm for brown $RuH(CO)(PCyc_3)_2(AL\text{-}H)$. Absorbance spectral data for these complexes are presented in Table 5.

Representative electronic absorption spectra are shown in Figure 5. Absorbance spectral features around and below 300 nm can be attributed to various intraligand and/or interligand transitions; the lower energy absorption bands, however, are attributed to MLCT transitions. Figure 6 presents steady-state fluorescence spectra for the same compounds dissolved in dichloromethane. The remainder of our presentation here focuses on the properties of $Ru(CO)_2(PBu_3)_2(AL\text{-}2H)$ exclusively because it exhibited the strongest luminescence. The electronic absorbance spectra of $Ru(CO)_2(PBu_3)_2(AL\text{-}2H)$ dissolved in seven different solvents are presented in Figure 7. A careful examination of the spectra reveals that the molar absorptivities, in general, increase as the solvent dipolarity decreases. More

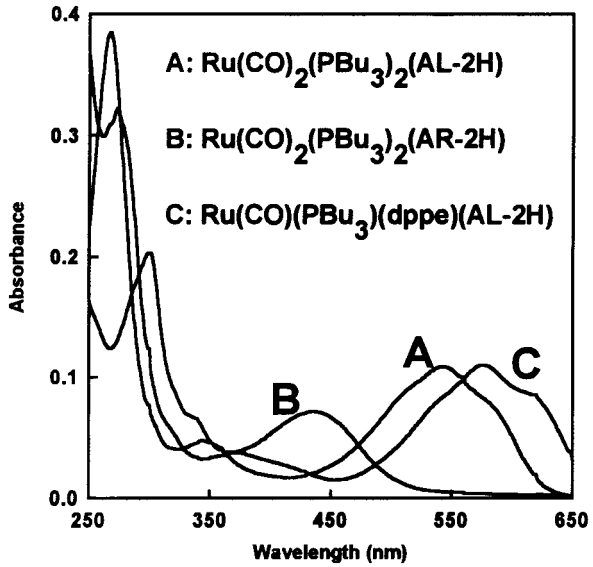

Figure 5. Absorbance spectra of dilute dichloromethane solutions of $Ru(CO)_2(PBu_3)_2(AL\text{-}2H)$, $Ru(CO)_2(PBu_3)_2(AR\text{-}2H)$, and $Ru(CO)(PBu_3)(dppe)(AL\text{-}2H)$.

vibronic structure is also evident for the compound in the nonpolar solvents such as cyclohexane and toluene, while these features vanish as the solvent dipolarity increases. Furthermore, there is also a bathochromic shift in the low-energy absorbance maximum as the solvent dipolarity increases. Table 6 reports the low-energy absorbance maxima and the corresponding decadic molar absorptivities of $Ru(CO)_2(PBu_3)_2(AL\text{-}2H)$ dissolved in the solvents studied.

Figures 8 and 9 show the relative and normalized fluorescence emission spectra, respectively, for 5 μM $Ru(CO)_2(PBu_3)_2(AL\text{-}2H)$ dissolved in the degassed solvents studied. The emission maxima are reported in Table 6. A blue shift in emission maximum is observed with a decrease in the solvent dipolarity, suggesting an increase in the $Ru(CO)_2(PBu_3)_2(AL\text{-}2H)$ dipole moment in the excited state relative to the ground state.[27,28]

(27) Lippert, V. E. *Z. Electrochem.* **1957**, *61*, 962.

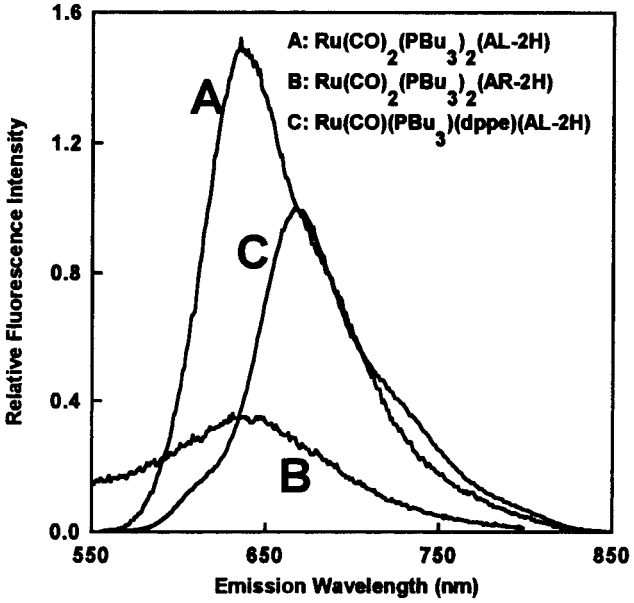

Figure 6. Fluorescence spectra of dilute solutions of $Ru(CO)_2(PBu_3)_2$-(AL-2H) (λ_{exc} = 543 nm; excitation and emission spectral band-passes at 8 and 4 nm, respectively), $Ru(CO)_2(PBu_3)_2$(AR-2H) (λ_{exc} = 436 nm, excitation and emission spectral band-passes at 16 and 16 nm, respectively), and Ru(CO)(dppe)(PBu_3)(AL-2H) (λ_{exc} = 543 nm; excitation and emission spectral band-passes at 16 and 8 nm, respectively).

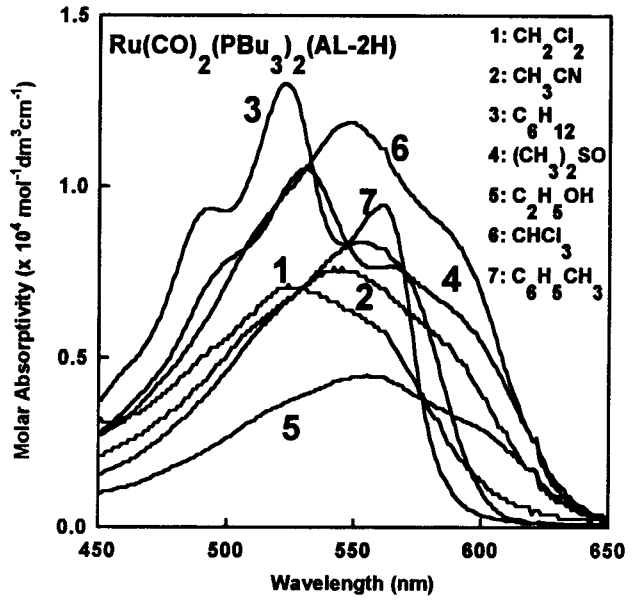

Figure 7. Molar absorptivities of $Ru(CO)_2(PBu_3)_2$(AL-2H) in seven different solvents.

If we assume that $Ru(CO)_2(PBu_3)_2$(AL-2H) exhibits a cavity radius of 6 Å,[29,30] a Lippert analysis[27,28] of the data presented in Table 6 yields estimates of the difference between the excited- and ground-state dipole moments ($\Delta\mu$) of 5−6 D. This change in dipole moment demonstrates that there is a significant change in the electronic configuration of $Ru(CO)_2(PBu_3)_2$(AL-2H) upon optical excitation.

(28) Mataga, N.; Kaifu, Y.; Koizumi, M. *Bull. Chem. Soc. Jpn.* **1956**, *29*, 465.
(29) Birks, J. B. *Photophysics of Aromatic Molecules*, Wiley-Interscience: New York, 1970.
(30) Lakowicz, J. R. *Principles of Fluorescence Spectroscopy*, Plenum Press: New York, 1983.

Table 6. Absorbance and Fluorescence Maxima and Molar Absorptivities for $Ru(CO)_2(PBu_3)_2$(AL-2H) in Various Solvents

solvent, dielectric constant	absorbance max, nm[a]	fluorescence max, nm[a]	log ϵ (dm^3 mol^{-1} cm^{-1})[b]
cyclohexane, 2.02	522	594	4.11
toluene, 2.38	530	600	4.02
chloroform, 4.81	547	632	4.07
dichloromethane, 8.93	544	635	3.85
dimethyl sulfoxide, 47.24	552	645	3.92
ethanol, 25.3	555	641	3.65
acetonitrile, 36.64	542	636	3.88

[a] ±1 nm. [b] ±0.1.

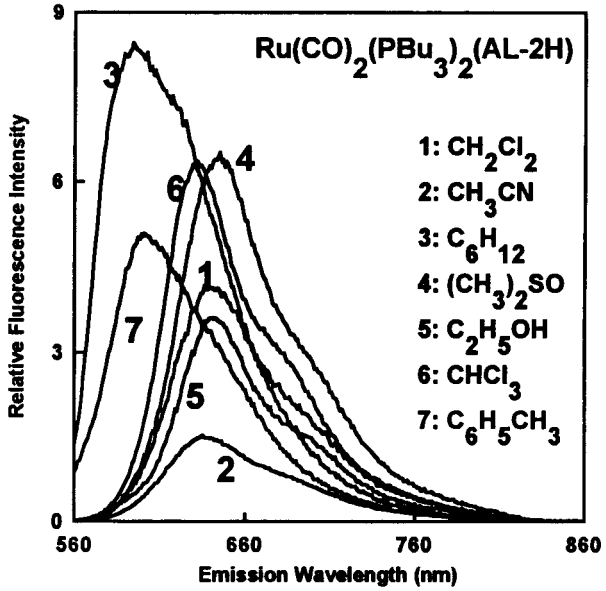

Figure 8. Fluorescence spectra of $Ru(CO)_2(PBu_3)_2$(AL-2H) in seven different solvents (λ_{exc} = 543 nm; excitation and emission spectral band-passes at 8 and 4 nm, respectively).

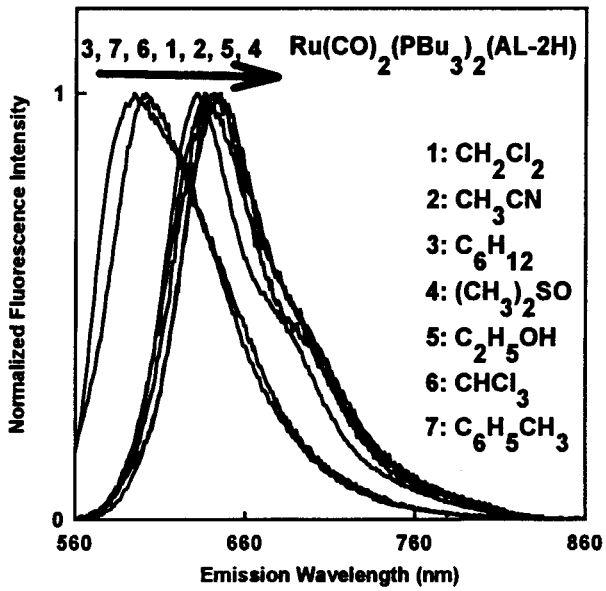

Figure 9. Normalized fluorescence spectra of $Ru(CO)_2(PBu_3)_2$(AL-2H) in seven different solvents (λ_{exc} = 543 nm; excitation and emission spectral band-passes at 8 and 4 nm, respectively).

Table 7 reports the fluorescence quantum yields, excited-state fluorescence lifetime, and the rates of radiative and nonradiative decays for $Ru(CO)_2(PBu_3)_2$(AL-2H) dissolved in the solvents studied. These results show that the quantum yields for $Ru(CO)_2(PBu_3)_2$(AL-2H) are between 2- and 20-fold less than

Table 7. Fluorescence Quantum Yields (Φ), Excited-State Lifetimes (τ), Radiative Decay Rates (k_r), and Nonradiative Decay Rates (Σk_{nr}) for $Ru(CO)_2(PBu_3)_2$(AL-2H) Dissolved in Various Solvents at Ambient Temperature

solvent	Φ^a	τ, ns[b]	$10^7 k_r$, s^{-1}	$10^9 \Sigma k_{nr}$, s^{-1}
cyclohexane	0.002	0.22	0.81 ± 0.08	4.54 ± 0.41
toluene	0.005	0.28	1.74 ± 0.15	3.55 ± 0.25
chloroform	0.018	1.08	1.68 ± 0.09	0.91 ± 0.02
dichloromethane	0.014	1.03	1.33 ± 0.07	0.96 ± 0.01
dimethyl sulfoxide	0.014	1.05	1.34 ± 0.07	0.94 ± 0.01
ethanol	0.010	0.84 ± 0.01	1.19 ± 0.06	1.18 ± 0.01
acetonitrile	0.010	0.98 ± 0.01	1.07 ± 0.05	1.01 ± 0.01

[a] ± 0.001. [b] $\leq \pm 0.02$ ns.

those for $Ru(bpy)_3^{2+}$. They also show that the excited-state fluorescence lifetimes are between 2 and 3 orders of magnitude less than those of $Ru(bpy)_3^{2+}$. Finally, the results presented in Table 7 show that the k_r and Σk_r values differ by about 1−2 orders of magnitude.

The origin of the significantly shorter (a factor of 10^3) excited-state fluorescence lifetimes for $Ru(CO)_2(PBu_3)_2$(AL-2H) relative to other luminescent ruthenium complexes such as $Ru(bpy)_3^{2+}$, $Ru(dpp)_3^{2+}$, and related compounds arises from the unique molecular structure of this complex, including the lack of symmetry inherent to the other aforementioned ruthenium complexes as well as the nonaromaticity of four of the ligands. As is well-documented,[31−33] the emitting-state energies and excited-state photophysical properties are sensitive to variations in the metal, coordinating ligand, and physicochemical properties of the local environment. In fact, solvents and substituent choices may be used to control the relative energetics of different excited states and to tune the photophysical and photochemical properties of these sorts of Ru-based luminophores (cf. Tables 6 and 7). Many of these complexes exhibit a diversity of energetically accessible charge-transfer, ligand-field, and intraligand excited states. These excited states have different orbital parentages and, thus, quite different excited-state characteristics.[31−33]

The low-energy absorbance bands can be attributed to the MLCT states; the fluorescence maxima above and around 600 nm are also consistent with the formation of MLCT excited states. However, the MLCT excited states here are very different from those of $Ru(bpy)_3^{2+}$ and other related complexes. It is likely that the excited states for $Ru(CO)_2(PBu_3)_2$(AL-2H) are either significantly mixed versions of MLCT, ligand-field, and intraligand states or that intersystem crossings are considerably enhanced, perhaps due to the presence of the PBu_3 ligands. From a photophysical standpoint, $Ru(CO)_2(PBu_3)_2$(AL-2H) is unique in the origin of its behavior and in its potential bioanalytical utility.

Acknowledgment. Research contributions from Mr. Mark Przybylski and Ms. Sinduja Srinivasan are gratefully acknowledged. This work was funded in part by a grant from the Petroleum Research Fund (to J.B.K.), administered by the American Chemical Society, and by grants to F.V.B. from the National Science Foundation, the Office of Naval Research, and the Department of Energy.

Supporting Information Available: Listings of crystal data, crystallographic data collection information, structure solution, and refinement details, atomic coordinates and equivalent isotropic displacement coefficients, bond lengths, bond angles, anisotropic displacement coefficients, hydrogen atom coordinates and isotropic displacement coefficients, along with a packing diagram of the molecules within the unit cell (Figure 1S). This material is available free of charge via the Internet at http://pubs.acs.org.

IC000529X

(31) Xu, W.; McDonough, R. C., III.; Langsdorf, B.; Demas, J. N.; Degraff, B. A. *Anal. Chem.* **1994**, *66*, 4133.
(32) Demas, J. N.; Degraff, B. A. *Anal. Chem.* **1991**, *63*, 829A.
(33) Juris, A.; Balzani, V.; Barigelletti, F.; Campagna, S.; Belser, P.; von Zelewsky, A. *Coord. Chem. Rev.* **1988**, *84*, 85.